Thermochimica Acta, 51 (1981) 153—168
Elsevier Scientific Publishing Company, Amsterdam — Printed in The Netherlands

THERMAL STABILITY AND PHASE TRANSITIONS OF THE OXIDES OF ANTIMONY

S.E. GOLUNSKI, T.G. NEVELL and M.I. POPE

Department of Chemistry, Portsmouth Polytechnic, Portsmouth (Gt. Britain)

(Received 9 May 1981)

ABSTRACT

This paper describes a study of the range of thermal stability and phase transitions in the following oxides of antimony: orthorhombic and cubic Sb_2O_3, orthorhombic Sb_2O_4 and cubic Sb_2O_5. The main thermoanalytical technique used has been DTA, in conjunction with TG, thermodilatometry and measurement of electrical conductivity. Our results show that orthorhombic Sb_2O_3 melts reversibly when heated in nitrogen; cubic Sb_2O_3 first undergoes an irreversible phase transition at approximately the same temperature, to give the orthorhombic allotrope, which then immediately melts. Oxidation of orthorhombic Sb_2O_3 in air commences at a significantly lower temperature than that of the cubic form, the product in both cases being orthorhombic Sb_2O_4. This latter compound is stable in atmospheres ranging from pure oxygen to nitrogen at temperatures exceeding 1000°C. Cubic Sb_2O_5 loses oxygen progressively on heating above 400°C, leading eventually to the formation of orthorhombic Sb_2O_4. However, while X-ray diffraction confirms that the latter structure has been formed by 750°C, evolution of oxygen continues up to 900°C, by which temperature the expected stoichiometric loss in mass is achieved.

INTRODUCTION

The oxides of antimony are of considerable importance in the preparation of catalysts for the selective partial oxidation of hydrocarbons. However, both the chemical structure and the phase composition of these mixed oxide catalysts have a pronounced effect on their activity and selectivity.

Two compounds have been identified in the system uranium—antimony—oxygen [1], these are USb_3O_{10} and $USbO_5$. Both catalysts show a high degree of activity in the oxidation of alkenes, but the former is much more selective with respect to the formation of partial oxidation products.

Far more work has been published on bismuth molybdate catalysts (which also show high activity in the selective partial oxidation of alkenes) than on the corresponding uranium antimonate system. In particular, the Bi_2O_3—MoO_3 phase diagram has been determined [2] and several kinetic studies carried out [3—7]. The role of chemisorbed and of lattice oxygen in the reaction mechanism has also been elucidated [8,9]. Determination of the phase diagram for the U—Sb—O system has not yet been achieved, since this necessarily requires an understanding of the interaction between the known compounds and phases in the systems Sb—O and U—O.

0040-6031/81/0000—0000/$02.75

Some of the published data relating to the former system appear to be open to serious doubt. For example, it has been reported [10] that DTA of Sb_2O_3 indicated that an exothermic transition occurred during heating in nitrogen, or argon, whereas the corresponding process occurring in air gave rise to an endothermic peak. Such a result is highly unlikely and also conflicted with our preliminary studies. Similar concern has been expressed by Cody et al. [11], who have clarified many of the previously existing problems. However, these workers did not carry out any DTA or electrical conductivity measurements; both techniques are particularly well suited to the study of solid—solid phase transitions.

Some of the difficulty in interpreting earlier data on Sb_2O_3 is almost certainly due to the existence of two allotropic forms, both of which are stable at room temperature. Orthorhombic Sb_2O_3 is known as valentinite and cubic Sb_2O_3 as senarmontite; separation of the allotropes is essential if meaningful results are to be obtained. Antimony tetroxide, Sb_2O_4, normally occurs only in the orthorhombic (α) form called cervantite, although a high temperature monoclinic (β) allotrope can be prepared [12,13].

The pentoxide, Sb_2O_5, is known to exist in a cubic form, while the sample studied by Cody et al. [11] was shown to be hydrated. An oxide corresponding to the formula Sb_6O_{13} has been reported [11] as being formed as an intermediate in the decomposition of Sb_2O_5 to Sb_2O_4, in the temperature range 650—850°C.

Accordingly we have investigated the thermal stability and phase composition of the oxides of antimony by means of DTA, TG, electrical conductivity measurements (ETA) and thermodilatometry (TD). Care has been taken to ensure that all materials used are both chemically pure and structurally homogeneous. Later we intend to extend this work to the study of phase equilibria in the U—Sb—O system, at atmospheric pressure.

EXPERIMENTAL

Differential thermal analysis (DTA) was carried out using a Standata 6-25, with heat treated alumina as the reference material and a flowing gaseous atmosphere. Unless stated otherwise, the heating rate used was 10 K min^{-1} and the sample mass was typically 60 mg.

A Stanton TG750 thermal balance was used for thermogravimetry (TG). Measurements were carried out in a flowing gaseous atmosphere, with a heating rate of 15 K min^{-1}, using samples weighing about 10 mg. Changes in mass could be determined to an accuracy of ca. ±0.1 mg.

Changes in the electrical conductivity (ETA) and linear dimensions (thermodilatometry, TD) of compacted samples were determined up to 1000°C, using an apparatus previously described [14]. Compaction was carried out using a stainless steel die and a hydraulic force of 10 tonnes, giving compacts 10 mm in diameter and about 5 mm in length. Electrical conductivity measurements were made using a Wayne Kerr B642 bridge, operating at a frequency of 1592 Hz; contact with the cylindrical oxide samples was made by platinum disc electrodes. ETA curves were obtained by plotting the logarithm

of the measured conductivity against reciprocal absolute temperature. The energy gap (E_g) between valence and conduction bands was calculated from the slope of rectilinear portions of the ETA curves, the slope corresponding to $-E_g/2kT$, where k is Boltzmann's constant.

X-Ray diffraction (XRD) powder photographs were taken to determine the crystal structure and composition of oxide samples before and after heat treatment. Samples were contained in glass capillary tubes and irradiated for 20 h with Cu$K\alpha$ X-rays; the resulting diffraction patterns were identified by comparison with standard data from the ASTM index.

Infrared absorption spectroscopy (IR) has been used to characterize our antimony trioxide samples and to confirm assignments made by XRD. Spectra were obtained using a Perkin-Elmer 577 spectrophotometer and KBr discs containing 3 wt.% antimony trioxide. Cubic Sb_2O_3 exhibits characteristic IR peaks at 745 and 385 cm^{-1}, while orthorhombic Sb_2O_3 shows an equally significant peak at 690 cm^{-1} [15]. Changes in the relative heights of these peaks have previously been used [16] to study the kinetics of the phase transition.

MATERIALS

Several commercial samples of antimony trioxide were purchased and investigated using such techniques as IR and XRD. The most satisfactory material was "Puratronic" Sb_2O_3, supplied by Alpha Chemicals (Ventron, Lancaster Synthesis Ltd.), described as being 99.999% pure on a metal basis and having a density of 5.67 g cm^{-3}. (Literature values [17] for the density of cubic and orthorhombic Sb_2O_3 are 5.2 and 5.67 g cm^{-3}, respectively.) However, even this material contained a small amount of cubic Sb_2O_3, which was eliminated by melting and re-solidifying under nitrogen. Subsequent examination by IR showed that characteristic absorption peaks due to the cubic form (745 and 385 cm^{-1}) were absent, while those resulting from orthorhombic Sb_2O_3 (690, 585, 540, 460 and 325 cm^{-1}) were clearly apparent. Comparison of the XRD powder pattern of the re-solidified melt with ASTM index 11-689 confirmed that the product was orthorhombic Sb_2O_3.

Cubic Sb_2O_3 was prepared from Alfa "Puratronic" Sb_2O_3 by sublimation under vacuum (<0.01 Torr), followed by condensation of the vapour on a water cooled glass surface. The resulting crystals were characterized by their IR spectrum (principal peaks occurring at 950, 740—720 and 385 cm^{-1}) and by the correspondence between the XRD powder pattern and ASTM index 5-0534.

"Ultrapure" orthorhombic Sb_2O_4 (stated density 5.82 g cm^{-3}) and "Puratronic" Sb_2O_5 (stated density 3.80 g cm^{-3}) were both supplied by Alpha Chemicals. XRD and IR confirmed that the tetroxide was in the pure orthorhombic form; this was indistinguishable from the cooled residue obtained by heating Sb_2O_3 in air at 1000°C.

The IR spectrum of Sb_2O_5 closely resembled that of orthorhombic Sb_2O_4, while XRD did not reveal evidence of any impurities.

RESULTS AND DISCUSSION

Orthorhombic Sb_2O_3, valentinite

(a) In flowing nitrogen

On heating in a flowing nitrogen atmosphere, the first thermal effect to be observed was a change in slope of the ETA plot (Fig. 1a) at about 225°C, which was not reflected by any of the other techniques used (cf. Fig. 2). Similar increases in electrical conductivity have been observed with other oxides in this region of temperature and can be ascribed to loss of chemisorbed hydroxyl groups. The resulting weight loss is too small to show up on the TG curve.

The original "Puratronic" material and the re-solidified melt both gave remarkably similar ETA plots, showing five rectilinear regions below the melting point. None of the changes in slope correlates directly with observable physical, or chemical transitions in the bulk structure. However, the very rapid increase in conductivity with temperature occurring above 550°C is accompanied by marked contraction of the sample (Fig. 2c).

DTA (Fig. 2a) exhibits only one, sharp, endothermic peak in the tempera-

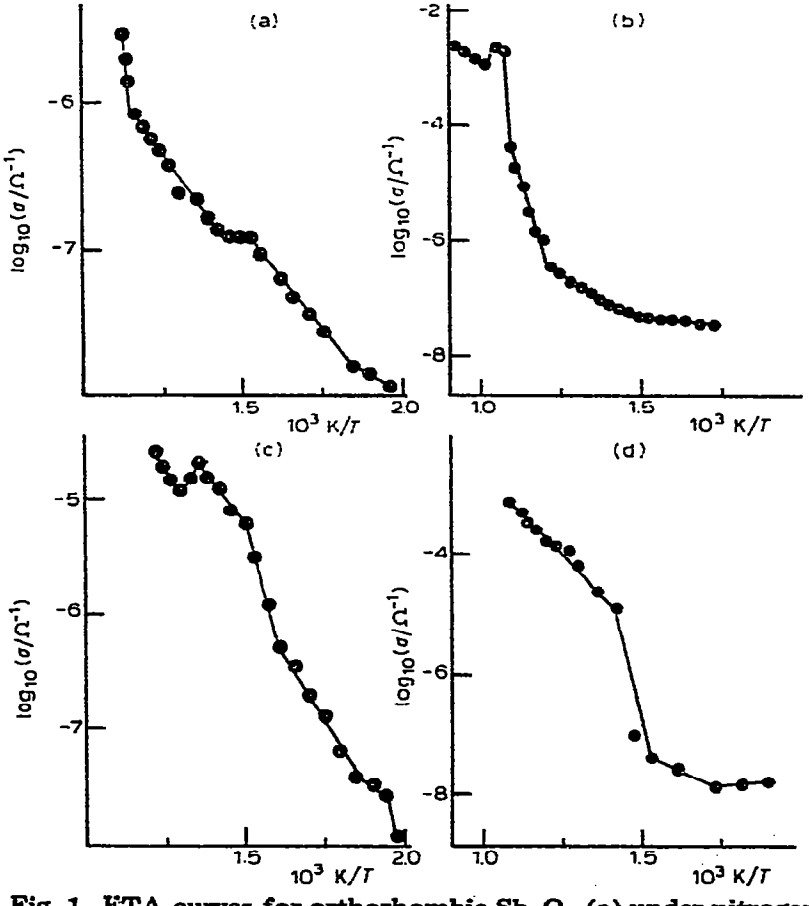

Fig. 1. ETA curves for orthorhombic Sb_2O_3 (a) under nitrogen and (b) under oxygen; for cubic Sb_2O_3 (c) under nitrogen and (d) under oxygen.

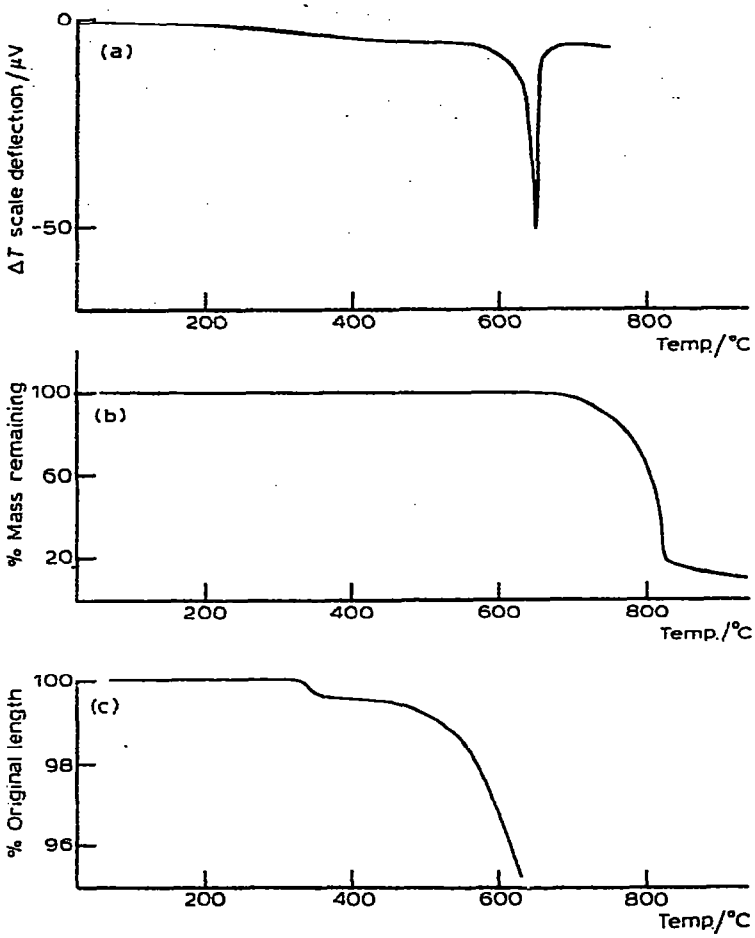

Fig. 2. Thermal analysis of orthorhombic Sb_2O_3 under nitrogen. (a) DTA: gas flow rate 500 cm^3 min^{-1}; heating rate 10°C min^{-1}. (b) TG: gas flow rate 200 cm^3 min^{-1}; heating rate 15°C min^{-1}. (c) TD: gas flow rate 500 cm^3 min^{-1}; heating rate 5°C min^{-1}.

ture range studied; this has an extrapolated onset temperature (T_e) of 628°C and a peak temperature (T_p) of 643 ± 2°C. On cooling, a much smaller exothermic peak having an identical T_e value was observed. XRD and IR showed that the cooled material was neither physically nor chemically changed. TG (Fig. 2b) indicated that a progressive loss in weight occurred above 625°C, reaching 90% by 1000°C.

It is therefore clear that, in an inert atmosphere, orthorhombic Sb_2O_3 melts at 628°C and that the resulting liquid progressively volatilizes. There is no evidence of chemical decomposition below 1000°C.

(b) In flowing air

From inspection of Figs. 1b and 3 it is at once apparent that orthorhombic Sb_2O_3 behaves very differently when heated in air, instead of nitrogen. The DTA curve exhibits a large, irreversible exotherm, T_e, occurring at 463°C, while the shape of the TG curve (Fig. 3b, c) was dramatically influenced by the changes in the experimental conditions. TD showed that samples con-

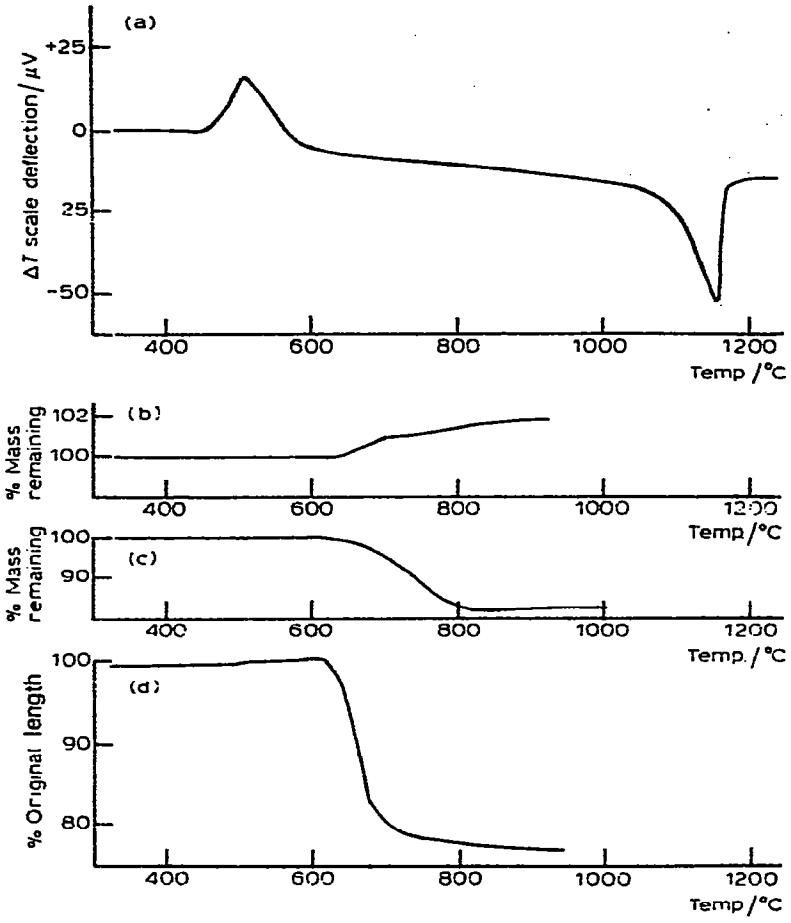

Fig. 3. Thermal analysis of orthorhombic Sb_2O_3 under air and oxygen. (a) DTA under air: gas flow rate 500 cm^3 min^{-1}; heating rate 10°C min^{-1}. (b) TG under oxygen: gas flow rate 100 cm^3 min^{-1}; heating rate 5°C min^{-1}. (c) TG under air: gas flow rate 200 cm^3 min^{-1}; heating rate 15°C min^{-1}. (d) TD under oxygen: gas flow rate 500 cm^3 min^{-1}; heating rate 5°C min^{-1}.

tracted by ca. 23% of their original length (Fig. 3d) over the temperature range 600—700°C.

Evidence from IR and XRD confirms that orthorhombic Sb_2O_3 is converted into orthorhombic Sb_2O_4 over the temperature range 500—700°C. The ETA plot (Fig. 1b) showed clear changes in slope at 410, 560 and 640°C; the slope of the curve above 700°C led to an E_g value of 1.54 eV, which is close to that obtained (1.59 eV) for orthorhombic Sb_2O_4 over the same range of temperature. Hence our conclusions are in general agreement with those of Gopalakrishnan and Manohar [18]. Variations in the TG plots with experimental conditions are attributed to competition between oxidation (causing a weight gain) and loss in weight due to volatilization of unreacted Sb_2O_3.

Further heating above 1000°C gave rise to a large, single, endothermic peak on the DTA curve (Fig. 3a), having a T_e value of 1105°C. It thus appears

that orthorhombic Sb_2O_4 is stable in air up to a considerably higher temperature than that recorded [17] in a standard reference source (930°C).

Cubic Sb_2O_3, senarmontite

(a) In flowing nitrogen

It is apparent from the ETA plot that changes in the sample occur at temperatures well below those observable by DTA or TG. As with orthorhombic Sb_2O_3, the slope of the ETA plot (Fig. 1c) increases above 230°C; further changes in slope were observed at 350 and 530°C. This latter temperature coincides with the onset of progressive contraction of the sample (Fig. 4d).

The first perceptible loss in weight by cubic Sb_2O_3 only became apparent at about 640°C (Fig. 4c). A double endothermic peak appeared on the DTA curve (Fig. 4a) at a similar temperature, followed by a continuing endother-

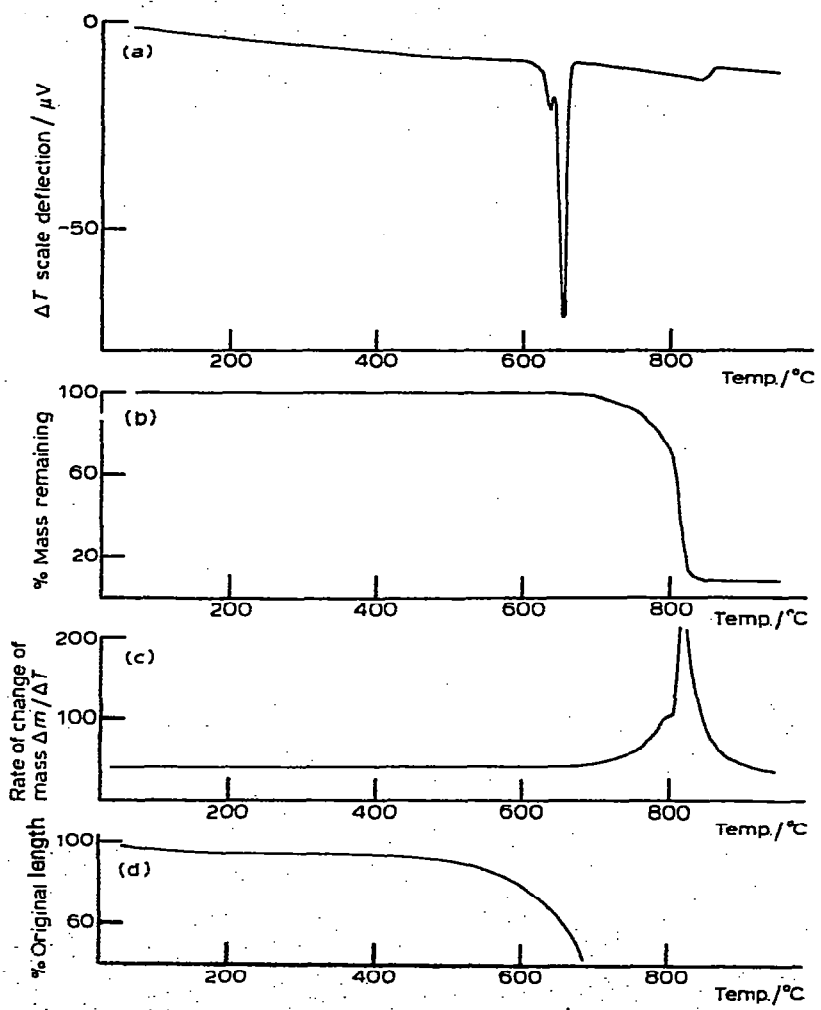

Fig. 4. Thermal analysis of cubic Sb_2O_3 under nitrogen. (a) DTA: gas flow rate 500 cm^3 min^{-1}; heating rate 10°C min^{-1}. (b) TG: gas flow rate 200 cm^3 min^{-1}; heating rate 15°C min^{-1}. (c) DTG: gas flow rate 200 cm^3 min^{-1}; heating rate 15°C min^{-1}. (d) TD: gas flow rate 500 cm^3 min^{-1}; heating rate 5°C min^{-1}.

mic drift. Both peaks are sharp and the first (T_e 629°C, T_p 639°C) was shown to be irreversible. That this irreversible endotherm was due to the cubic orthorhombic solid state phase transition was shown by IR spectroscopy. Figure 5 illustrates the spectrum of cubic Sb_2O_3 as prepared (a) and after heating to 640°C (b); the virtual disappearance of the characteristic cubic phase absorption peak at 385 cm^{-1} will at once be apparent. This finding was confirmed by XRD.

The second endothermic peak, having an observed onset temperature of 643 ± 2°C and a T_p value of 651 ± 2°C, was clearly reversible. This endotherm is attributed to the melting of orthorhombic Sb_2O_3 immediately following its formation. No ETA or TD measurements could be made above this temperature, but DTG (Fig. 4c) indicated the onset of a progressive loss in weight at ca. 640°C, resulting from vaporization of molten Sb_2O_3. Vaporization is also reflected by the continuing endothermic drift of the DTA curve, which subsequently returns to the baseline at about 840°C. Termination of the DTG peak occurs at about 860°C, showing that no further volatile material remained. The total recorded weight loss of the DTA sample at this temperature was 99.7%; TG indicated a slightly smaller loss in weight, but it was subsequently observed that some crystals had condensed on cooler parts of the apparatus.

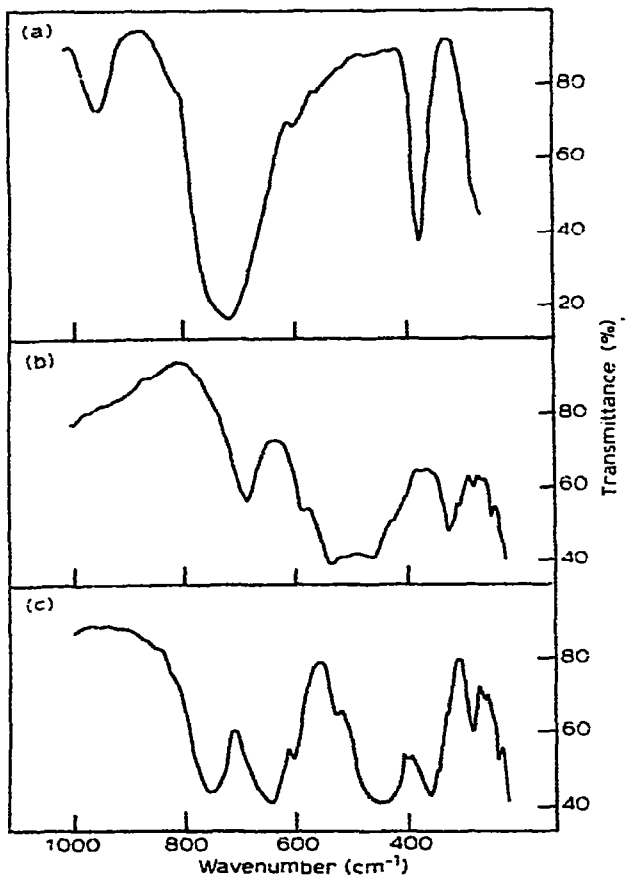

Fig. 5. IR absorption spectra of cubic Sb_2O_3. (a) As prepared; (b) after heating to 640°C under nitrogen; (c) after heating to 800°C under air.

It is interesting to note that the DTG peak exhibits a distinct shoulder, suggesting that two concurrent processes are involved. This is in accordance with the observations of Cody et al. [11] who ascribe their double peak to sublimation of the solid and boiling of molten Sb_2O_3.

(b) In flowing air

On heating cubic Sb_2O_3 in an oxygen containing atmosphere, a sharp change in slope in the ETA curve (Fig. 1d) occurs in the region of 375°C. This probably corresponds to the similar effect observed at ca. 350°C in flowing nitrogen. A second change in slope at 435°C is due to some effect which was not recorded by any of the other thermoanalytical techniques employed. The pellet broke up at about 640°C, due to stresses resulting from oxidation.

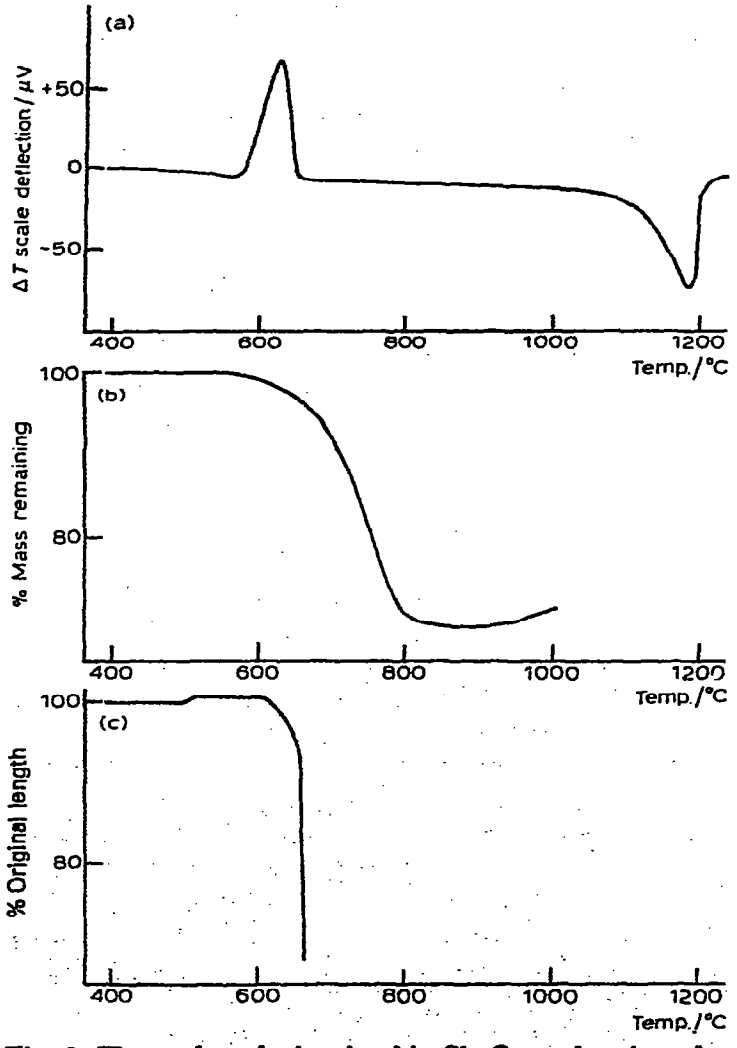

Fig. 6. Thermal analysis of cubic Sb_2O_3 under air and oxygen. (a) DTA gas flow rate 500 cm^3 min^{-1}; heating rate 10°C min^{-1}.(b) TG under air: gas flow rate 200 cm^3 min^{-1}; heating rate 15°C min^{-1}. (c) TD under oxygen: gas flow rate 50 cm^3 min^{-1}; heating rate 5°C min^{-1}.

Onset of oxidation first became apparent on the DTA curve (Fig. 6a), giving rise to a large exothermic peak with an extrapolated onset temperature of 575°C and a T_p value of 630°C. The TG curve is more difficult to interpret, because any weight gain due to the formation of Sb_2O_4 is more than offset by loss in weight resulting from volatilization of unreacted Sb_2O_3 (Fig. 6b). Rapid contraction of the sample took place above 600°C.

Further heating in air leads eventually to a large endothermic peak on the DTA curve, T_e 1103°C. This peak has already been ascribed to dissociation of orthorhombic Sb_2O_4 to form Sb_2O_3 and oxygen, followed immediately by vaporization of the former. IR spectroscopy of a sample of cubic Sb_2O_3 heated in air to 800°C showed (Fig. 5c) strong absorption bands at 750, 645, 445 and 365 cm^{-1}. This, together with the XRD powder pattern, confirms that the oxidation product is orthorhombic Sb_2O_4.

It is interesting to note that the greater thermal stability of cubic Sb_2O_3, as indicated by its higher melting point, is also reflected in the temperature at which oxidation first became apparent, viz. 575°C as against 463°C for orthorhombic Sb_2O_3. Thermodynamic calculations predict that the cubic form should indeed be slightly more stable, since the free energies of formation of cubic and orthorhombic Sb_2O_3, at 500°C, are —498.0 kJ $mole^{-1}$ and —497.5 kJ $mole^{-1}$, respectively [17].

Orthorhombic (α) Sb_2O_4, cervantite

This compound is remarkably stable and on heating in either flowing nitrogen, or in air, gave rise to no thermal effects on the DTA curve below about 1000°C, nor to any detectable weight loss (Fig. 7). A change in slope of the ETA curve (Fig. 8a) occurred at about 330°C, accompanied by substantial contraction of the sample between 300 and 350°C. This temperature range corresponds closely to the Tamman temperature of orthorhombic Sb_2O_4, so that the enhanced electrical conductivity can probably be ascribed to lattice diffusion of ions [19]. Above 350°C a rectilinear ETA graph was obtained, with a slope corresponding to an E_g value of 1.59 eV; this figure agrees well with those derived from samples of Sb_2O_3 heated in air.

Above 1000°C, the DTA curve exhibits a large endothermic peak, which in nitrogen has a T_e value of 1063°C; a similar peak occurs in air, but with a slightly higher onset temperature. It has been suggested that orthorhombic Sb_2O_4 sublimes at a temperature of between 950 and 1050°C, the actual value depending on the method of preparation. To test this hypothesis, DTA was carried out in controlled atmospheres, ranging in composition from pure nitrogen to pure oxygen. It was found that the extrapolated onset temperature of the endothermic peak increased progressively with increasing oxygen content of the atmosphere, reaching 1168°C in pure oxygen. Such behaviour is inconsistent with volatilization and strongly suggests that dissociation of Sb_2O_4 to Sb_2O_3 is involved, as reported by Cody et al. [11].

$$\alpha Sb_2O_4(s) \rightarrow Sb_2O_3(s) + 0.5\ O_2(g)$$

$$Sb_2O_3(s) \rightarrow [Sb_2O_3(1)] \rightarrow Sb_2O_3(g)$$

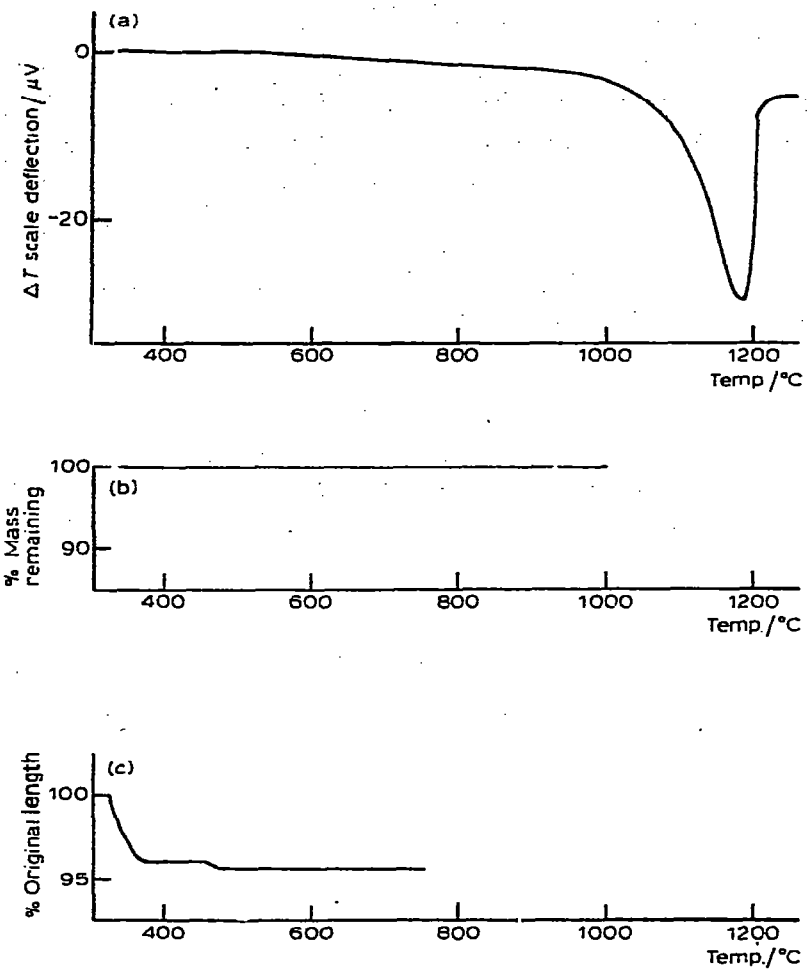

Fig. 7. Thermal analysis of α-Sb_2O_4 under nitrogen. (a) DTA: gas flow rate 500 cm^3 min^{-1}; heating rate 10°C min^{-1}. (b) TG: gas flow rate 200 cm^3 min^{-1}; heating rate 15°C min^{-1}. (c) TD gas flow rate 500 cm^3 min^{-1}; heating rate 5°C min^{-1}.

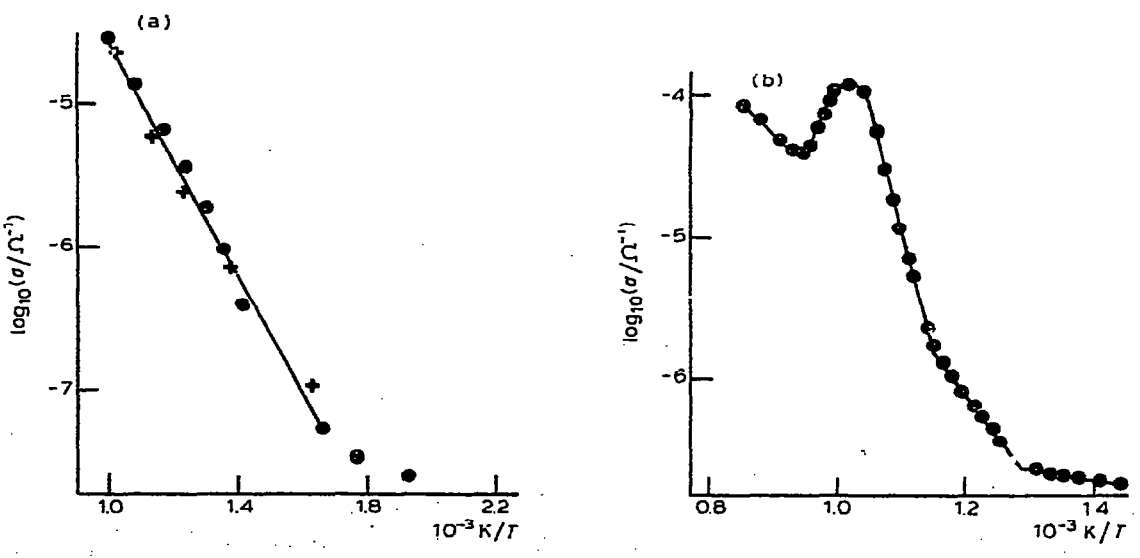

Fig. 8. ETA curves for (a) α-Sb_2O_4 under nitrogen, and (b) Sb_2O_5 under nitrogen. ●, Heating; +, cooling.

Now the observed onset temperature of the DTA peak would be expected to relate to the first of these two consecutive steps, for which the equilibrium constant, K_p, can be written

$$K_p \simeq P_{O_2}^{1/2}$$

P_{O_2} is the partial pressure of oxygen in equilibrium with the sample. Since the variation of K_p with temperature is given by the equation

$$\ln K_p = \frac{-\Delta H}{RT} + \text{constant}$$

it should be possible to evaluate the enthalpy change, ΔH, accompanying the reaction, from the slope of a graph of $\ln P_{O_2}^{1/2}$ plotted against reciprocal absolute temperature. That the data do indeed give a rectilinear plot is shown in Fig. 9; the value of ΔH obtained from the slope of the graph is 206 kJ mole^{-1}.

Calculation of enthalpy changes at 1400 K, using tabulated thermodynamic data [17], yields values of +173 kJ mole^{-1} for the formation of solid orthorhombic Sb_2O_3 and +232 kJ mole^{-1} if the product is formed in the liquid state. Hence the enthalpy change obtained by DTA falls midway between these two estimated values.

Cubic Sb_2O_5

As with orthorhombic Sb_2O_4, the shape of the DTA curve was virtually unaffected by changing from flowing nitrogen to flowing air. A small, irreversible, exothermic peak (Fig. 10a) was observed, the T_e value of which was not highly reproducible; the experimental temperatures obtained ranged

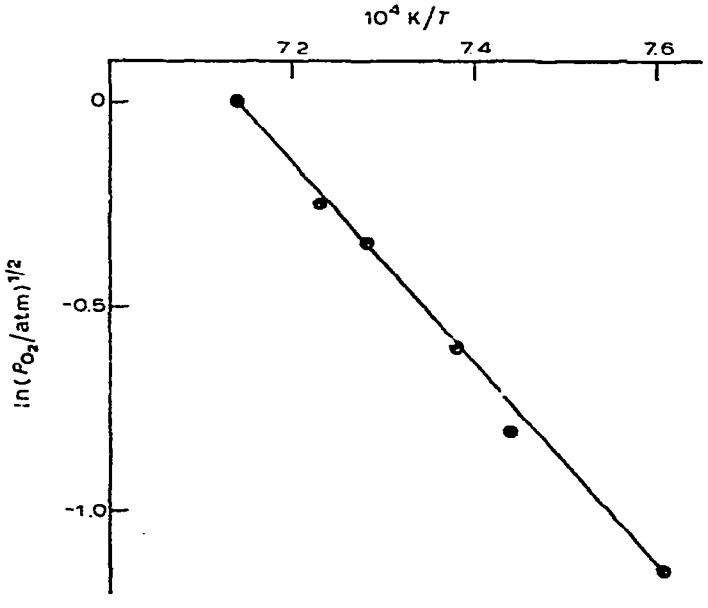

Fig. 9. Dependence on oxygen pressure of the onset temperature of the DTA peak for the decomposition of α-Sb_2O_4.

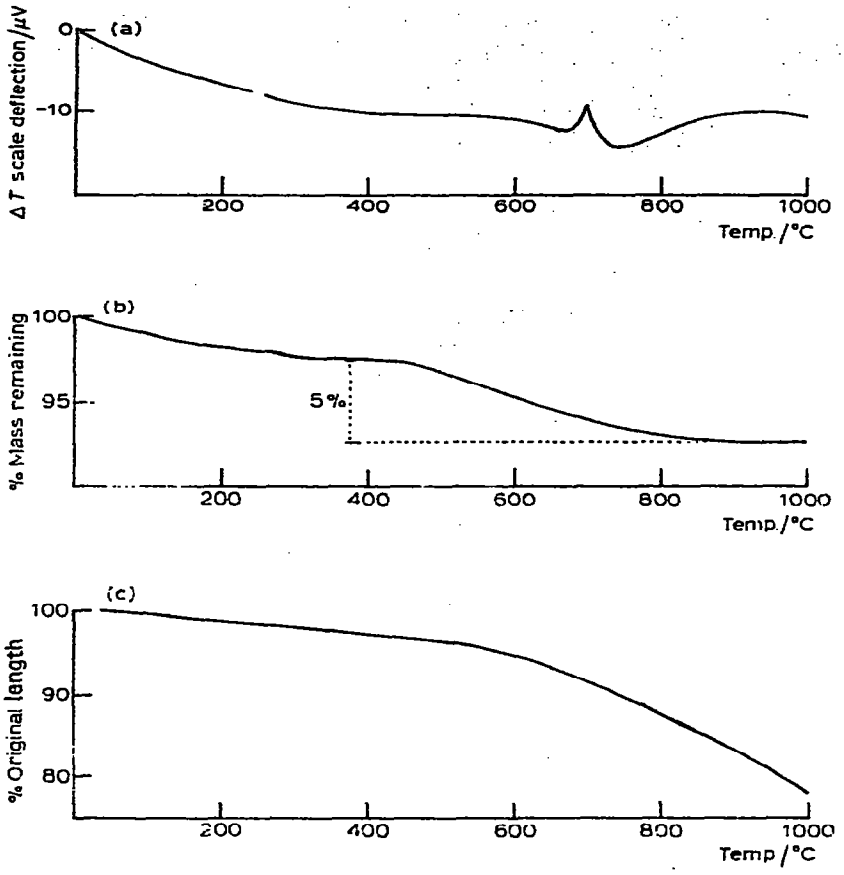

Fig. 10. Thermal analysis of Sb_2O_5 under nitrogen. (a) DTA: gas flow rate 500 cm^3 min^{-1}; heating rate 10°C min^{-1}. (b) TG: gas flow rate 200 cm^3 min^{-1}; heating rate 15°C min^{-1}. (c) TD: gas flow rate 500 cm^3 min^{-1}; heating rate 5°C min^{-1}.

between 650 and 680°C. That this exotherm was due to dissociation of Sb_2O_5 to form orthorhombic Sb_2O_4 was confirmed by XRD powder photographs, which are shown in Fig. 11. Figures 11a and b correspond to Sb_2O_5 as supplied and after heating to 620°C in nitrogen, respectively; the two XRD patterns are clearly identical. Pattern 11c differs markedly from 11b and represents Sb_2O_5 after heating to 750°C in nitrogen. This photograph is indistinguishable from that obtained (11d) for Sb_2O_3 heated in air to 800°C, resulting in the formation of orthorhombic Sb_2O_4.

DTA of Sb_2O_5 above 750°C led only to the characteristic dissociation endotherm of orthorhombic Sb_2O_4, discussed in the preceding section.

The dissociation of Sb_2O_5 to Sb_2O_4 showed up clearly on the ETA curve (Fig. 8b). Over the temperature range 600—660°C a rectilinear plot was obtained; then from 660 to 780°C the conductance actually decreased with increasing temperature. Above 780°C a rectilinear graph was again recorded, giving a value of 1.57 eV for E_g. This figure is in close agreement with that previously recorded (1.59 eV) for orthorhombic Sb_2O_4.

The evidence from TG (Fig. 10b) is surprising, because the sample of Sb_2O_5 shows a continuing loss in weight between 400 and 900°C, the total weight loss being 5.0%. This figure agrees closely with the calculated weight

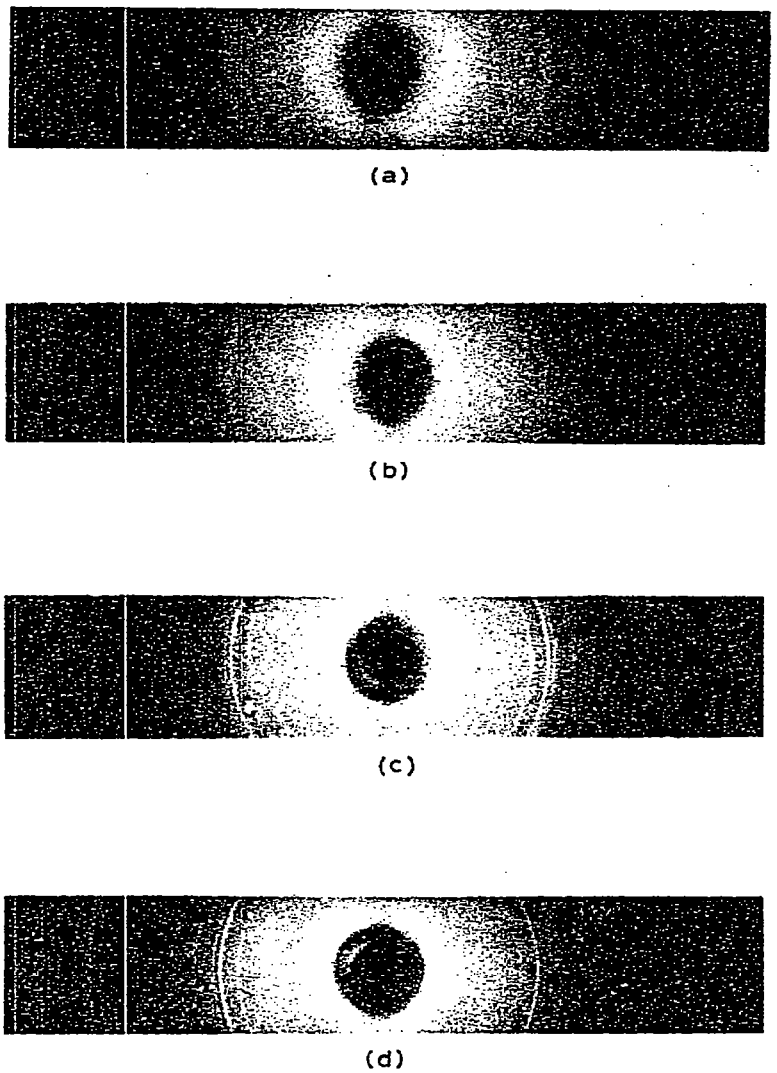

Fig. 11. X-Ray powder diffraction photographs. (a) Untreated Sb_2O_5; (b) Sb_2O_5, after heating to 620°C under nitrogen; (c) Sb_2O_5, after heating to 750°C under nitrogen; (d) α-Sb_2O_4, prepared by heating Sb_2O_3 to 800°C under air.

loss (4.95%) for the formation of Sb_2O_4, but does not explain the marked effects shown by DTA and ETA in the region 650—700°C. It therefore appears that gradual depletion of oxygen eventually leads to crystallization of the new oxide phase, confirmed by XRD, even though a considerable stoichiometric excess of oxygen over that expected for Sb_2O_4 still remains in the lattice.

Substantial contraction of the sample would be expected to accompany the conversion of Sb_2O_5 to Sb_2O_4, since the density of the reactant (3.80 g cm^{-3}) is much less than that of the product (5.82 g cm^{-3}). However, the TD curve (Fig. 10c) is consistent with TG in showing no sudden change in sample dimensions in the region 650—700°C. Instead, progressive contraction of the sample occurs above about 400°C and continues at least up to 1000°C.

Since our sample of Sb_2O_5 contained no water of hydration, unlike that of

Cody et al. [11], results from the two studies are not really comparable. Nevertheless, we could find no evidence to support the formation of an intermediate oxide having the formula Sb_6O_{13}. In particular, our DTA curves give no indication of any transition occurring between 850 and 890°C, which is the temperature range over which Sb_6O_{13} is reported to convert to orthorhombic Sb_2O_4.

The effect of heating Sb_2O_5 in flowing nitrogen can therefore be expressed as

$$\text{cubic } Sb_2O_5 \xrightarrow{650\text{—}700^\circ C} \text{orthorhombic } Sb_2O_4$$

the product is unaffected by further heating below 1000°C.

CONCLUSION

Valentinite, orthorhombic Sb_2O_3, melts reversibly at 628°C when heated in flowing nitrogen; further heating leads only to volatilization of the melt.

Senarmontite, cubic Sb_2O_3, does not melt, but undergoes a solid phase transition at essentially the same temperature (629°C) to give solid valentinite, which immediately melts.

On heating in flowing air, or oxygen, both crystal forms of Sb_2O_3 oxidize to orthorhombic Sb_2O_4; however, oxidation of valentinite was first apparent at 463°C, while senarmonite remained stable up to 575°C.

Cervantite, orthorhombic (α) Sb_2O_4, was found not to undergo any physical or chemical change on heating below 1000°C, either in air or nitrogen. Above 1000°C, cervantite dissociated into Sb_2O_3 and oxygen, the onset temperature of the reaction increasing with partial pressure of oxygen in the surrounding atmosphere. The enthalpy change for this reaction was determined from the onset temperature of the DTA endothermic peaks, giving a value of 206 kJ $mole^{-1}$. This figure was in reasonable agreement with the theoretical enthalpy changes calculated for the formation of liquid and solid orthorhombic Sb_2O_4, 232 and 173 kJ $mole^{-1}$, respectively. Our results show that orthorhombic Sb_2O_4 is stable in air well above 1000°C, a figure substantially in excess of that (930°C) quoted in reference tables [17].

As with cervantite, Sb_2O_5 behaves very similarly when heated in nitrogen, or in air. Oxygen is lost progressively from the crystal structure above 400°C, leading eventually to a transition to orthorhombic Sb_2O_4, which is reflected in an irreversible exothermic DTA peak and a sudden fall in electrical conductivity with increasing temperature. This transition occurs in the region 650—680°C and has been shown by X-ray diffraction to be complete by 750°C. However, oxygen continues to be lost up to 900°C, at which temperature the total weight loss corresponds to the stoichiometric value expected for the formation of Sb_2O_4.

Our sample of Sb_2O_5 clearly differs from that of Cody et al. who showed conclusively that their oxide was hydrated. We found no evidence for the formation of Sb_6O_{13} as an intermediate decomposition product; nor could we find any indication of a transition occurring between 850 and 890°C, which is the temperature range where Sb_6O_{13} would be expected to form

orthorhombic Sb_2O_4 [11]. However, it does appear that the orthorhombic Sb_2O_4, formed by heating Sb_2O_5 to 750°C, contains a stoichiometric excess of oxygen.

Our data do not support the information cited in a standard reference book [17], which states that Sb_2O_5 loses one oxygen atom at 380°C and a second at 930°C.

REFERENCES

1 R.K. Grasselli and D.D. Suresh, J. Catal., 25 (1972) 273.
2 M. Egashira, M. Katsuo, S. Kagawa and T. Seiyama, J. Catal., 58 (1979) 409.
3 C.R. Adams, Proc. 3rd Int. Congr. Catal., Amsterdam, 1 (1964) 240.
4 G.W. Keulks, J. Catal., 19 (1970) 232.
5 K.M. Sancier, P.R. Wentrcek and H. Wise, J. Catal., 39 (1975) 141.
6 T. Otsubo, H. Miura, Y. Morikawa and T. Shirasaki, J. Catal., 36 (1975) 240.
7 M. Kobayashi and R. Futaya, J. Catal., 56 (1979) 73.
8 J.M. Peacock, A.J. Parker, P.G. Ashmore and J.A. Hockey, J. Catal., 15 (1969) 387.
9 E.V. Hoefs, J.R. Monnier and G.W. Keulks, J. Catal., 57 (1979) 331.
10 Y.K. Agrawal, A.L. Shashimohan and A.B. Biswas, J. Therm. Anal., 7 (1975) 635.
11 C.A. Cody, L. Dicarlo and R.K. Darlington, Inorg. Chem., 18 (1979) 1572.
12 D. Rogers and A.C. Skapski, Proc. Chem. Soc., (1964) 400.
13 A.C. Skapski and D. Rogers, Chem. Commun., 23 (1965) 611.
14 M.D. Judd and M.I. Pope, J. Appl. Chem., 20 (1970) 380.
15 O. Borgen and J. Krogh-Moe, Acta Chem. Scand., 10 (1956) 265.
16 P.S. Gopalakrishnan and H. Manohar, J. Solid State Chem., 15 (1975) 61.
17 Handbook of Chemistry and Physics, The Chemical Rubber Co., Cleveland, 59th edn., 1978, p. B97.
18 P.S. Gopalakrishnan and H. Manohar, Curr. Sci., 38 (1969) 306.
19 S.J. Gregg, The Surface Chemistry of Solids, Chapman and Hall, London, 2nd edn., 1965, p. 158.